05,11

Topological features of the electronic structure and phase diagram of the chiral ferromagnet MnSi

© A.A. Povzner, A.G. Volkov, M.A. Chernikova

Ural Federal University after the first President of Russia B.N. Yeltsin,
Yekaterinburg, Russia

E-mail: a.a.povzner@urfu.ru

Received August 28, 2023
Revised October 16, 2023
Accepted October 19, 2023

It is shown that the reason for the appearance of the complex pattern of chiral spin short-range order observed in the helical ferromagnet MnSi is a topological electronic transition (TET). TET occurs under conditions of thermodynamic instability of ferromagnetism, when the mode-mode parameter in the Ginzburg-Landau functional becomes negative, and the chemical potential falls into the energy region of Berry curvature. It was found that the topological features of the electronic structure lead to the appearance of skyrmion lattices phases and fluctuations of left-chiral spin helices. In the paramagnetic region, a phase of fluctuations of left- and right-handed spin spirals appears. The emergence of a thermodynamically stable non-chiral paramagnetic phase is accompanied by a shift in the chemical potential beyond the energy region of Berry curvature and an abrupt disappearance of local magnetization (delayed magnetic phase transition). The constructed $h-T$ phase diagram (h is the magnetic field strength, T is the temperature) is consistent with experiment.

Keywords: Berry phases, fluctuations, chiral spin spirals, skyrmions.

DOI: 10.61011/PSS.2023.12.57688.189

1. Introduction

MnSi manganese monosilicide is one of the most studied prototypes of spintronic materials with a B20 type crystal structure, in which there is no inversion center [1–3]. The ferromagnetic state of the MnSi spin subsystem is chiral because, along with the exchange interaction, an antisymmetric Dzyaloshinsky-Moriya (DM) exchange occurs in it. In the paper of Jansen-Bak [4] it was shown that the competition of the DM-interaction with the inhomogeneous exchange interaction leads to the occurrence of ferromagnetic long-period spin spirals with a wave vector $\mathbf{q}_0$, at that the transition from the helicoid ferromagnetic phase to paramagnetic phase is not a second-order phase transition. As was shown in [5], that one of the reasons for the disruption of the second-order transition is the interaction of spin fluctuations with phonon fluctuations.

On the other hand, analysis of the results of DFT-calculations of the electronic structure shows [6,7] that a significant enhancement of zero spin fluctuations occurs in the ground state of MnSi. The temperature increasing of thermal fluctuations leads to the suppression of zero fluctuations [6]. As a result, there is a change in the sign of the mode-mode parameter, which, according to the Ginzburg-Landau model [8], shall lead to thermodynamic instability of chiral ferromagnetism to a first-order magnetic phase transition.

However, the nature of the resulting phase transition remains unclear. In particular, the reasons, why the observed phase transition is accompanied by the appearance of the topological Hall effect (THE) [9], were not fully identified. Moreover, it was noted in [9,10] that the reason for the THE appearance in MnSi is the topological features of the electronic structure associated with the Berry curvature on its Fermi surface.

The experimentally established $h-T$-diagram of magnetic states of MnSi (see, for example, [1]), along with the regions of helical ferromagnetic spirals and magnetic field-induced ferromagnetism, also contains phases of skyrmion lattices and fluctuations of spin spirals. In this case, it should be supplemented by taking into account the unusual intermediate phase with partial spin chirality discovered during small-angle scattering of polarized neutrons [11].

To clarify the nature of phase transitions that occur with changes in temperature and magnetic field, in particular leading to the formation of a phase with partial spin chirality, it is necessary to develop a spin-fluctuation approach to the study of chiral band ferromagnetism, taking into account the topological features of the electronic structure. In this paper, such approach is developed on the basis of the interpolation spin-fluctuation theory of band magnetism [12]. Taking into account the concepts of MnSi electronic structure, resulting from *ab initio* GGA modeling, the topological nature is clarified of phases of chiral spin short-range order in the $h-T$-diagram of the chiral ferromagnet under study.

2. Model

Let us consider the Hubbard Hamiltonian (H) for strongly correlated electrons of a chiral ferromagnet, in which we take into account the topological features of

the electronic spectrum in the term of the Hamiltonian responsible for the band motion (H_0). In this case, along with the term of the intra-atomic Coulomb repulsion (δH_U) with the Hubbard interaction parameter (U), we will consider the antisymmetric spin-spin DM interaction (δH_D). Then

$$H = H_0 + \delta H_U + \delta H_D, \quad (1)$$

where

$$H_0 = \sum_{\mathbf{k},\sigma} \varepsilon_{\mathbf{k}} a^+_{\mathbf{k},\sigma} a_{\mathbf{k},\sigma},$$

Moreover, the topological features of the spectrum d-electrons $\varepsilon_{\mathbf{k}}$ are taken into account in the DFT approximation;

$$\delta H_U = U \sum_{\mathbf{q}} \left(4^{-1}|\delta n_q|^2 - |S^{(z)}_q|^2\right)$$

— Hamiltonian of the Hubbard interaction, written through the spin and charge density operators;

$$\delta H_D = \sum_{\mathbf{q}} \mathbf{h}^{(D)}_{\mathbf{q}} \mathbf{S}_{-\mathbf{q}}$$

— DM interaction Hamiltonian, presented in the mean field approximation $\mathbf{h}^{(D)}_{\mathbf{q}} = -id[\mathbf{M}_{\mathbf{q}} \times \mathbf{q}]$ (Dzyaloshinsky field), in which d — DM interaction constant, $\mathbf{M}_{\mathbf{q}} = \langle \mathbf{S}_{\mathbf{q}} \rangle$ — vector of the Fourier transform of the inhomogeneous magnetization of a spin configuration with a wave vector $\mathbf{q}$;

$$S^{(z)}_{\mathbf{q}} = \sum_{\sigma} \sigma n_{\mathbf{q},\sigma}/2, \;\; \delta n_{\mathbf{q}} = \sum_{\sigma} n_{\mathbf{q},\sigma} - \delta_{\mathbf{q},0} n,$$

$$n_{\mathbf{q},\sigma} = \sum_{\mathbf{k}} a^+_{\mathbf{k},\sigma} a_{\mathbf{k}+\mathbf{q},\sigma}, \;\; a^+_{\mathbf{k},\sigma} (a_{\mathbf{k},\sigma})$$

— birth (annihilation) operators of d-electron in a state with quasi-momentum $\mathbf{k}$and spin quantum number σ, n — number of d-electrons per site Mn.

Let's write the partition function of the considered dynamical system of strongly correlated d-electrons in the Matsubara representation [13]:

$$Z = \mathrm{Sp} T_\tau \exp\left(-\int_0^\beta H(\tau) d\tau\right),$$

where $\beta = 1/T$, T — temperature in energy units, T_τ — Matsubara time ordering operator τ, $H(\tau) = e^{H_0 \tau} H e^{-H_0 \tau}$.

For the thermodynamic potential, we will use the known thermodynamic relation $\Omega = T \ln Z$. At the same time, using the Stratonovich–Hubbard transformations [12], we reduce the original many-particle problem of the motion and interaction of d-electrons to description of their motion in fluctuating in space and time exchange ($\xi_\nu(\tau)$) and charge ($\eta_\nu(\tau)$) fields. As a result, additionally taking into account the Dzyaloshinsky fields, we have

$$\Omega = \Omega_0 + \Delta\Omega. \quad (2)$$

Here Ω_0 — thermodynamic potential of non-interacting electrons described by the Hamiltonian H_0;

$$\langle (\ldots) \rangle = \mathrm{Sp}\left\{(\ldots) \exp\left(\beta\Omega_0 - \int_0^\beta \left(H_0(\tau) - \mu \sum_q |n_q|^2\right)\right)\right\};$$

$$\Delta\Omega = T \ln\left\langle T_\tau \int (d\eta d\boldsymbol{\xi}) \exp\left[-\sum_q (|\boldsymbol{\xi}_q - \mathbf{h}^{(D)}_q/c|^2 + |\tilde{\eta}_q|^2) - (U/T)^{1/2} \sum_q (\delta n_q (i\tilde{\eta}_q/2) - \mathbf{S}_q \boldsymbol{\xi}_{-q})\right]\right\rangle_0, \quad (3)$$

$c = (UT)^{1/2}$; $q = (\mathbf{q}, \omega_{2n})$, ω_{2n} — Matsubara Bose frequency;$\tilde{\eta}_q = \eta_q(1 - \delta_{q,0})$;

$$(d\eta d\boldsymbol{\xi}) = d\boldsymbol{\xi}_0 \left[\prod_{q \neq 0, j} d\boldsymbol{\xi}^{(j)}_q d\eta^{(j)}_q\right],$$

$d\eta^{(j)}_q$ and $d\boldsymbol{\xi}^{(j)}_q$ — actual ($j = 1$), imaginary ($j = 2$) parts of Fourier images of the charge ($\eta_\nu(\tau)$) and vector of exchange ($\boldsymbol{\xi}_\nu(\tau)$) fields, respectively; $\mathbf{h}_q = (\mathbf{h}\delta_{q,0} + \mathbf{h}^{(D)}_{\mathbf{q}})\delta_{q,\mathbf{q}}$, $\mathbf{h}$ — homogeneous external magnetic field in units of two Bohr magnetons (μ_B).

Further, following the interpolation theory [12], we will split $\Delta\Omega$ into a homogeneous and inhomogeneous part (which corresponds to the gradient terms in the Ginzburg–Landau functional [8]). As a result, we get expression

$$\Omega = -T \ln \int_{-\infty}^{\infty} (d\boldsymbol{\xi}, d\eta) \exp\left(-\sum_q \left((1 - X_q)|\eta_q|^2 + (1 + X_q)|\boldsymbol{\xi}_q - c^{-1}\mathbf{h}_q|^2\right) - \Phi(\boldsymbol{\xi}, \eta)\right), \quad (4)$$

in which $\Phi(\boldsymbol{\xi}, \eta)$ — functional of the free energy of d-electrons moving in stochastic charge and exchange fields fluctuating in space and time

$$\Phi(\boldsymbol{\xi}, \eta) = \int_0^\beta d\tau \sum_{\mathbf{v}, \alpha(=\pm 1)} \int g_0(\varepsilon) \times \ln\left(1 + \exp T^{-1}\left(\mu - \varepsilon + \alpha c|\boldsymbol{\xi}_\nu(\tau)| + ic\tilde{\eta}_\nu\right)\right) d\varepsilon; \quad (5)$$

and the correction $X_q = U(\chi^{(0)}_0 - \chi^{(0)}_q)$, which takes into account the inhomogeneity of the isotropic exchange interaction, is determined through the Pauli susceptibility of d-electrons and is described by the Lindhard function [9]:

$$\chi^{(0)}_q = \chi^{(0)}_0 \left(1 - A\mathbf{q}^2 - iB \frac{\omega}{|q|}\right),$$

where the homogeneous static component $\chi^{(0)}_0$ corresponds to the density of d-states $g_0(\varepsilon)$ at $\varepsilon = \mu$ (chemical potential).

3. Equation of magnetic state

To estimate the functional integrals in the expression of the thermodynamic potential (4), we will use the procedure of the saddle-point method for the actual and imaginary parts of charge (with $q \neq 0$) and static (with $q = \mathbf{q}$) exchange fields η_q and $\xi_q^{(\gamma)}$; and also modulus of dynamic (with $\omega_{2n} \neq 0$) exchange fields: $|\xi_q^{(\gamma)}| = r_q^{(\gamma)}$, where γ — index of spatial coordinate axes.

At the same time, taking into account the connection between the saddle values of the exchange fields $\xi_{\mathbf{q}}^{(\gamma)}$ with the average values of the spin density operators, coinciding with the magnetization ($\mathbf{M}_q$), as well as the connection $r_q^{(\gamma)}$ with the root-mean-square amplitudes spin fluctuations [9], we obtain the equations of magnetic state in the form

$$M_0^{(z)}(D^{-1} + 2\kappa \sum_{\mathbf{q}} |\mathbf{M}_{\mathbf{q}}|^2)$$

$$+ 2\kappa \sum_{\mathbf{q}^{(1)},\mathbf{q}^{(2)},\mathbf{q}^{(3)}} M_{\mathbf{q}^{(1)}}^{(z)} (\mathbf{M}_{\mathbf{q}^{(2)}} \mathbf{M}_{\mathbf{q}^{(3)}}) \delta_{\sum_1^3 \mathbf{q}^{(1)}=0} = h/U, \quad (6a)$$

$$M_{\mathbf{q}}^{(\gamma)} \Big(D^{-1} + 2\kappa M_0^{(z)} + \kappa \sum_{\mathbf{q}^{(1)} \neq 0} |\mathbf{M}_{\mathbf{q}}^{(1)}|^2 + A\mathbf{q}^2 \Big)$$

$$+ \kappa \sum_{\mathbf{q}^{(1)},\mathbf{q}^{(2)},\mathbf{q}^{(3)} \neq 0} (\mathbf{M}_{\mathbf{q}^{(1)}} \mathbf{M}_{\mathbf{q}^{(2)}}) M_{\mathbf{q}^{(3)}}^{(\gamma)} (1 - \delta_{\mathbf{q}^{(3)},\mathbf{q}}) \delta_{\sum_{j=1}^3 \mathbf{q}^{(j)};\mathbf{q}}$$

$$= h_{\mathbf{q},\gamma}^{(D)}/(U), \quad (6b)$$

taking into account the exchange enhancement of band magnetism (with a factor D) and the interaction of spin modes with mode-mode parameters (κ):

$$D = (1 - U\chi_\perp + \kappa(\langle \delta \mathbf{M}^2 \rangle + \langle m^2 \rangle/3))^{-1}$$

and

$$\kappa = U(\chi_\perp - \chi_\parallel)/(2M^2).$$

Here

$$\chi_\perp = (2UM)^{-1} \sum_{\alpha=\pm 1} \alpha \int d\varepsilon f(\varepsilon - \mu - \alpha UM) g_0(\varepsilon)$$

and

$$\chi_\parallel = 2\Big(\sum_{\alpha=\pm 1} g_\alpha(\mu) \Big)^{-1} \prod_{\alpha=\pm 1} g_\alpha(\mu),$$

where

$$g_0(\varepsilon) = g_0(\varepsilon + \alpha UM),$$

$$g_\alpha^{(n)}(\mu) = (-1)^{n+1} \int_{-\infty}^{\infty} g_\alpha(\varepsilon)(d^{n+1} f(\varepsilon - \mu)/d^{n+1}\varepsilon) d\varepsilon,$$

correspond to the transverse and longitudinal susceptibility of electrons, $M = (M_0^2 + \langle \delta M^2 \rangle + \langle m^2 \rangle)^{1/2}$ — root mean square magnetic moment, the amplitude of dynamic spin fluctuations is determined by the expression coinciding with the fluctuation-dissipation theorem

$$\langle \mathbf{m}^2 \rangle = 2U^{-1} \sum_{\mathbf{q},\gamma} \int_0^\infty \Big(\frac{1}{2} + f_{\mathrm{B}}(\omega/T) \Big)$$

$$\times \operatorname{Im} \left(D^{-1} + 2\kappa(M) |M_{\mathbf{q},\gamma}|^2 + X_{\mathbf{q},\omega} \right)^{-1} d\omega, \quad (7a)$$

and the contribution of fluctuations of spin density waves (SDWs) arises, with the mean square amplitude

$$\langle \delta M^2 | \rangle = \sum_q |\mathbf{M}_{\mathbf{q}}|^2. \quad (7b)$$

The solutions for dynamic thermal and zero-spin fluctuations (7a) and for spatial fluctuations of SDW (7b) correspond to the saddle-point variables $|\xi_q^{(\gamma)}| = r_q^{(\gamma)}$.

The wave vector $\mathbf{q}_0$ of the realized spin configurations is determined from the conditions of the minimum thermodynamic potential and turns out to depend on the projections onto the coordinate axes of magnetization $M_{\mathbf{q}}^{(\gamma)}$:

$$q_0^{(x)} = |\mathbf{q}_0| \left(\frac{(M_{\mathbf{q}_0}^{(+)} M_{-\mathbf{q}_0}^{(-)})^{1/2}}{|\mathbf{M}_{\mathbf{q}_0}|^2} \right) \operatorname{Re} M_{+\mathbf{q}_0}^{(z)};$$

$$q_0^{(y)} = |\mathbf{q}_0| \left(\frac{(M_{\mathbf{q}_0}^{(+)} M_{-\mathbf{q}_0}^{(-)})^{1/2}}{|\mathbf{M}_{\mathbf{q}_0}|^2} \right) \operatorname{Im} M_{\mathbf{q}_0}^{(z)};$$

$$q_0^{(z)} = \pm |\mathbf{q}_0| \left(\frac{M_{\mathbf{q}_0}^{(+)} M_{-\mathbf{q}_0}^{(-)}}{|\mathbf{M}_{\mathbf{q}_0}|^2} \right), \quad (8)$$

where $|\mathbf{q}_0| = d/2AU$, $M_{q_0}^{(+)} = (M_{-q_0}^{(-)})^* = M_{q_0}^{(x)} + iM_{q_0}^{(y)}$ — circular components of the vector $\mathbf{M}_{q_0}$.

The equations of magnetic state can be solved numerically only, taking into account the features of the electronic spectrum and DOS of d-electrons. Moreover, to analyze the possibilities of the occurrence of thermodynamic and topological phases, information is necessary on the chemical potential μ dependence on temperature and magnetic field. The latter can be obtained from the saddle point condition for η_0 and the electroneutrality requirement for the number of s- and d-electrons

$$N_e = N_S + \sum_{\alpha=\pm 1} \int d\varepsilon f(\varepsilon - \mu + \alpha UM) g(\varepsilon), \quad (9)$$

where N_e — total number of electrons, N_S — number of s-electrons, $f(\varepsilon)$ — Fermi-Dirac function.

4. $h-T$-spin state diagram

We will perform a numerical analysis of the chiral spin states of MnSi using, when solving the equations of the magnetic state, the results of ab initio calculations of the electronic structure. Such calculations for the electronic spectrum and density of states (DOS) of electrons in this

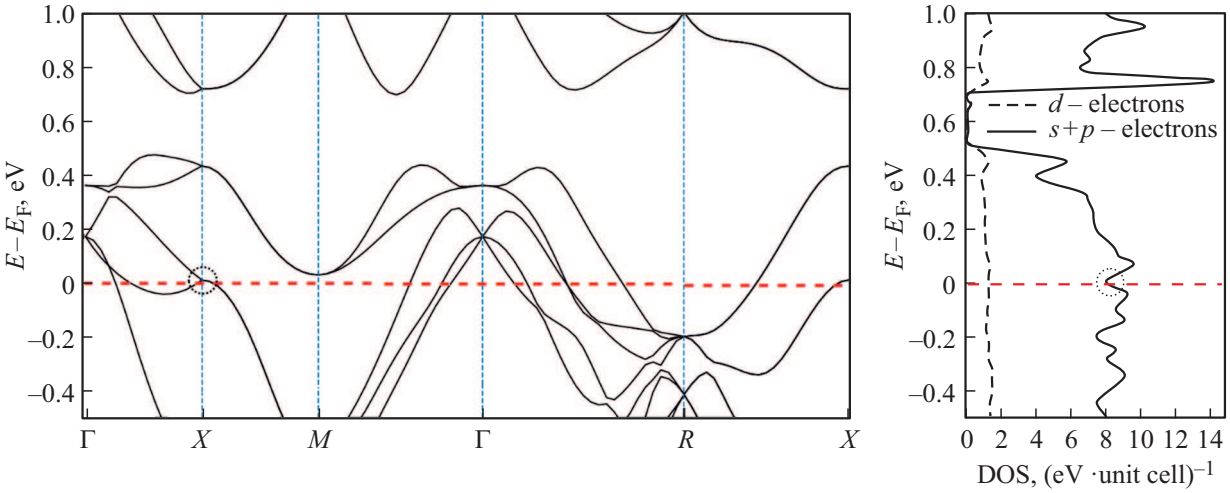

Figure 1. Electronic spectrum (left) and density of states of MnSi (right). The density of states (DOS) curve depicted by the solid line corresponds to d-electrons, and the dotted line corresponds to sp-electrons. The position of the Fermi level coincides with the origin of the energy reference. The energy region of Berry and DOS curvature is circled. Also circle marks the X-point of intersection of the branches at which Berry curvature occurs.

paper were performed taking into account the features of the MnSi crystal structure in the GGA approximation (Figure 1). The Elk code, which implements the full potential method of augmented plane waves, was used in the calculations. The exchange-correlation potential was chosen as GGA. The wave functions were taken on a grid of $16 \times 16 \times 16k$-points, and the cutoff length of the inverse wave vector G was set to 3.77 a.u.$^{-1}$.

The obtained results of DOS GGA calculations are in good agreement with those given in databases on topological materials [14]. However, they are insufficient to determine the temperature-field dependence of the mode-mode parameter, which, under the conditions of a temperature-prolonged phase transition in MnSi, is determined only after taking into account the features of the fine structure of DOS. Therefore, modeling of the fine structure of DOS of d-electrons in the energy range $|\varepsilon - \varepsilon_F| \leq 0.1$ eV was carried out, which led to the approximate expression

$$g(\varepsilon) = 147.05\varepsilon^6 + 61.9\varepsilon^5 - \varepsilon^4 - 19.9\varepsilon^3 - 6.96\varepsilon^2 + 0.21\varepsilon + 0.03,\ \text{eV}^{-1}.$$

The comparison of the modeling results of the fine structure of DOS with calculations of electronic spectra (Figure 1) shows that in the reviewed energy range, near the Fermi energy, there is an intersection of the branches of the electronic spectrum, leading to Berry degeneracy [10]. In this case, the DOS curvature, determined by its second derivative with respect to energy in the considered range, is negative.

The main results of the numerical analysis of solutions to the equations of magnetic state (6) in the considered model of the electronic structure are reduced to the following.

1. If the chemical potential determined by the electrical neutrality condition (9) is outside the Berry curvature of the electronic spectrum, and the value of the mode-mode interaction parameter is positive ($\kappa > 0$), then we obtain solutions corresponding to the spin helicoid with left-handed chirality

$$M_\nu^{(x)} = M_S \sin(\mathbf{q}_0 \boldsymbol{\nu}),$$
$$\nu^{(y)} = -M_S \cos(\mathbf{q}_0 \boldsymbol{\nu}), \quad M_\nu^{(z)} = \chi h. \tag{10}$$

Here the local magnetization

$$M_S^2 = (2\kappa)^{-1}\left(\left(D^{-1} + 2\kappa M_0^2 + X(\mathbf{q}_0, 0)\right)^2 - (d|\mathbf{q}_0|/U)^2\right)^{1/2}. \tag{11a}$$

magnetic susceptibility

$$\chi = 2U^{-1}\left(1 - (D^{-1} + 2\kappa M_0^2)^{-1}\right), \tag{11b}$$

and fluctuations of spin density waves (7b) are not observed: $\langle \delta M^2 \rangle = 0$.

In this case, just as during LDA+U+SO modeling in [6,7], the thermodynamically equilibrium chiral ferromagnetic state is realized only in the presence of zero spin fluctuations with a root-mean-square amplitude, which is comparable to the magnetization modulus $\mathbf{M_q}$. The condition for the existence of such solutions is determined by the inequality

$$D^{-1} + 2\kappa M_0^{(z)} < -3dq_0/4U.$$

The wave vector $\mathbf{q}_0$ of the helicoid (8) turns out to be fixed in absolute value (see (6))and perpendicular to the plane of the spiral in which the rotation occurs of xy-projection of local magnetization $\mathbf{M}_{\boldsymbol{\nu}}$. In the external uniform magnetic field perpendicular to the xy-plane, spin cones appear. In this case, the local magnetization acquires a z-component, and its x- and y-components decrease with the field $\mathbf{h}$ increasing.

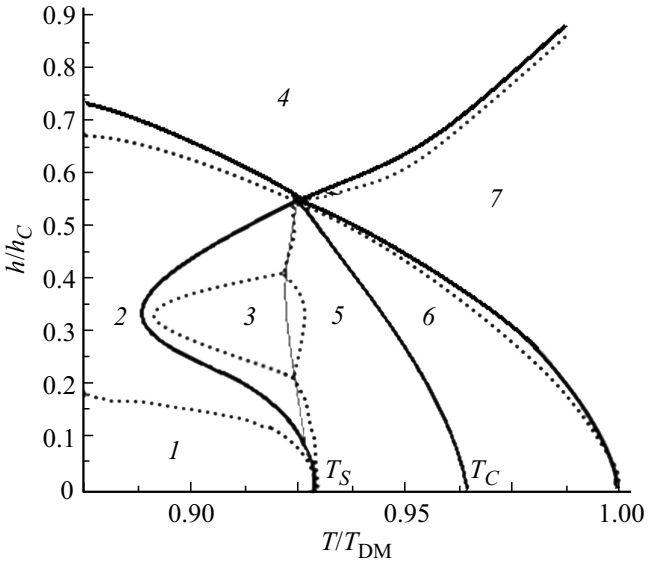

Figure 2. Phase diagram of MnSi. Solid lines — calculation results, dashed line — experiment data [1,15]. *1* — helicoidal (spiral) magnetism, *2* — helicoidal cone, *3* — skyrmion A-phase, *4* — field-induced **h** ferromagnetism, *5* — ferromagnetic helicoidal fluctuation disorder, *6* — paramagnetic helicoidal disorder, *7* — paramagnetism. The calculated values of the magnetic field of the helicoidal cone „collapse" at $T \to 0$ $\mu_{\mathrm{B}} h_C = 0.60T$ are used. The horizontal axis shows in relative units the calculated values of the temperature $T_S = 0.93T_{\mathrm{DM}}$ of the formation of left-hand chiral ferromagnetic fluctuations of spin spirals and the temperature of the formation of paramagnetic spin liquid with mixed (right-hand and left-hand) spin chirality — $T_C = 0.96T_{\mathrm{DM}}$. $T_{\mathrm{DM}} = 31.08\,\mathrm{K}$ — the calculated value of the temperature of the chirality disappearance and the paramagnetism appearance at $h = 0$. The calculations use the parameters $U = 0.93\,\mathrm{eV}$, $A = 0.07$ and $B = \pi/2.45$ from [16,17].

On the phase diagram we calculated (Figure 2), these solutions to the equations of magnetic state (11) describe phase 1.

In the external magnetic field $h > h_C$, where the critical field h_C is determined by the condition

$$2\kappa M_0^2(h_C) = -D^{-1} - \frac{3d|\mathbf{q}_0|}{U},$$

the helicoidal cone „collapses" and field-induced ferromagnetism occurs (phase 2).

2. Analysis of the electrical neutrality condition and solutions to the magnetic state equation shows that a change in the mode-mode parameter at temperature-field offset of the chemical potential to the region with negative DOS curvature leads to the suppression of zero fluctuations. In this case, the amplitude of the root-mean-square moment becomes small. As a result, for the parameters of mode-mode interaction and exchange enhancement, we approximately have

$$\kappa \approx U^3\big(g^{-1}(\mu)(g^{(1)}(\mu))^2 - g^{(2)}(\mu)\big)$$

and

$$D_0 \approx (1 - U\chi_0^{(0)})^{-1}. \quad (12)$$

According to (12) κchanges sign when the chemical potential shifts to the region of negative DOS curvature without changing the sign of the exchange enhancement parameter. Since the chemical potential shifts to the energy region of Berry curvature, TEP is induced in the system.

As a result of TEP, along with weak thermal spin fluctuations, topologically determined spatial fluctuations of SDW (7b) and fluctuations of charge fields η with a mean square $\langle\delta\eta^2\rangle = N_0^{-1}\sum_\nu(\eta_\nu - \nu_0)^2$ arise:

$$\langle\delta\mathbf{M}^2\rangle = \langle\delta\eta^2/4\rangle - \big[D_0^{-1} + \kappa\big(\mathbf{M}_0^2 + 5\langle m^2\rangle/3\big)\big]/\kappa, \quad (13a)$$

$$\left\langle\frac{\delta\eta^2}{4}\right\rangle = \langle\delta\mathbf{M}^2\rangle - \frac{[2 - D_0^{-1} - \kappa(\mathbf{M}_0^2 + \langle m^2\rangle)]}{\kappa}. \quad (13b)$$

According to the considered model of the electronic structure, if at $\kappa < 0$ and $D < 0$ the condition $D_0^{-1} - 2|\kappa|M_0^2 < -3d|\mathbf{q}_0|/4U$ is satisfied, then for the magnetic field induction $b < \frac{d|\mathbf{q}_0|M_S}{4}$ the solutions to the equations (6) describe a skyrmion lattice

$$M_\nu^{(x)} \cong M_S\cos(q_{0,i}\nu + \phi),\ M_\nu^{(y)} \cong M_S\sin(q_{0,i}\nu + \Phi),$$

$$M_\nu^{(z)} = |M_{q_0}^{(z)}|\cos(\mathbf{q}_{0,i}\boldsymbol{\nu} + \phi) + M_0^{(z)}, \quad (14a)$$

$$M_S^2 = (2|\kappa|)^{-1}\Big((D_0^{-1} - 2|\kappa|M_0^2 - |\kappa|(\langle\delta M^2\rangle - \langle\delta\eta^2/4\rangle) + X(\mathbf{q}_0, 0))^2 - (d|\mathbf{q}_0|/U)^2\Big)^{1/2}, \quad (14b)$$

The feature of skyrmion solutions is the occurrence of magnetization in the direction perpendicular to the plane of the spirals. However, according to estimates

$$|\mathbf{M}_{\mathbf{q}_0}^{(z)}|^2 = (4U)^{-2}(|\kappa|dq_0)^2\langle\delta\mathbf{M}^2\rangle - (h/U)^2 \ll M_S^2, \quad (15b)$$

due to which the spin configurations under consideration are quasiplanar.

According to the analysis of the terms of mode-mode coupling in the equation of magnetic state, the triple of wave vectors $q_{0,i}$ in expressions (14a) is equal to zero in sum. Therefore, the angle between adjacent wave vectors of spin modes $M_{\mathbf{q}}^{(\gamma)}$ is 120°, which, in accordance with [1,15], corresponds to the condition for the skyrmion lattice occurrence, which is the result of the superposition of three helical modes.

The calculated region of existence of the skyrmion phase 3 is shown in Figure 2. Phases 4 and 5 in the diagram we calculated (Figure 2) are also observed in experiment [1,15]. However, in contrast to [1,15], we show that one should distinguish between spin liquids with ferromagnetic and paramagnetic fluctuations of spin spirals.

Ferromagnetic fluctuations of spin spirals arise under the conditions both $0 > D_0^{-1} + 2\kappa M_0^{(z)} > -3dq_0/4U$ and

$\kappa < 0$, and are described by solutions of the magnetic state equation

$$M_{\boldsymbol{\nu}}^{(x)} = M_S \cos(\mathbf{q}_0 \boldsymbol{\nu} + \phi),$$

$$M_{\boldsymbol{\nu}}^{(y)} = M_S \sin(\mathbf{q}_0 \boldsymbol{\nu} + \phi), \; M_{\nu}^{(z)} = \chi h, \qquad (16)$$

in which stochastically changing phases ϕ appear. Just like for spin spirals (11), left-hand spin chirality is preserved here.

If the condition $0 < D_0^{-1} + 2\kappa M_0^2 < 3d|\mathbf{q}_0|/U$ and $\kappa < 0$ are satisfied, then phase 5 appears, which corresponds to the paramagnetic spin liquid with mixed (right-hand and left-hand) spin chirality. In this region, we obtain the following solutions to the equation of magnetic state

$$M_{\boldsymbol{\nu}}^{(x)} = M_S \cos(\mathbf{q}_0 \boldsymbol{\nu} + \phi),$$

$$M_{\boldsymbol{\nu}}^{(y)} = \pm M_S \sin(\mathbf{q}_0 \boldsymbol{\nu} + \phi), \; M_{\nu}^{(z)} = \chi h. \qquad (17)$$

Note that, as in the ordinary (non-chiral) paramagnetic state, in phase 5 the electron system is not magnetized at $h = 0$. However, in external magnetic field the magnetization proportional to h appears. The similar state of MnSi spin system was observed in experiments on small-angle scattering of polarized neutrons in [11], where mixed left-hand and right-hand spin chiralities were detected.

Note that chiral spiral modes $M_{\mathbf{q}}^{(y)}$ with fixed Berry phases shall be preserved within the correlation radii described by the expressions

$$R_C = 2\pi k_{\mathrm{F}}^{-1} (AU\chi)^{1/2}, \qquad (19)$$

where the magnetic susceptibility is

$$\chi = 2\chi_0^{(0)} \left(D_0^{-1} + \kappa (2M_0^2 + \langle \delta M^2 \rangle + 5\langle m^2 \rangle / 3) \right)^{-1}.$$

The estimates made taking into account the parameters of the electronic and magnetic subsystems [16,17] show that the value $R_C \approx 50$ angstrom, and weakly depends on the external magnetic field.

Finally, note that the non-chiral paramagnetic phase 6 (Figure 2) arises under conditions when, due to changes in temperature and magnetic field the chemical potential shifts beyond the Berry curvature region. In this case, a delayed magnetic phase transition to paramagnetic state takes place, it is accompanied by change in the negative sign of the mode-mode parameter to positive one, by the disappearance of spatial fluctuations of the electron density (13) and local magnetizations. Due to the disappearance of local magnetizations, the chiral effects of DM interaction also disappear.

5. Conclusion

Thus, we show that the topological features of the electronic structure lead to the appearance of topological magnetism phases on $h-T$ diagram of MnSi. The reason for the skyrmion phase, as well as phases with ferro- and paramagnetic chiral spin liquids occurrence is a topological electronic transition. In this case, TEP is caused by temperature- and external magnetic field-induced offset of the chemical potential of the electronic system into the region of Berry curvature.

TEP is accompanied by the appearance of spatial fluctuations of spin and charge density waves, which are the necessary condition for the topological magnetism formation. In this case, the comparison of the features of the electronic spectra leading to the Berry curvature with DOS features leads to the conclusion that the sign of the mode-mode parameter is related to the considered topological features of the electronic structure.

Since the degeneracy of electronic states associated with the Berry curvature is the cause of the topological Hall effect (THE) [9], as in accordance with the found phase diagram we can expect that even minor changes in the electronic structure will have a significant effect on THE. In particular, we expect that the experimental results describing the discovered THE [9] will be significantly supplemented after further, and primarily experimental its study on MnSi samples doped with various impurities.

Therefore, the study of topologically determined features of the fine electronic structure and spin correlations in chiral ferromagnets belonging to the B20 structure type is relevant for the further development of spintronic technologies.

Funding

The results were obtained as part of the assignment of the Ministry of Science and Higher Education, contract No. FEUZ-2023-0015.

Conflict of interest

The authors declare that they have no conflict of interest.

References

[1] A. Bauer, C. Pfleiderer. Springer Ser. Mater. Sci. **228**, 1–28 (2016).
[2] S.M. Stishov, A.E. Petrova. UFN **187**, *12*, 1365 (2017). (in Russian).
[3] S.M. Stishov, A.E. Petrova. UFN, **193**, 614 (2023). (in Russian).
[4] P. Bak, M.H. Jensen. J. Phys. C **13**, L1881 (1980).
[5] S.A. Pikin. JETP Lett. **106**, 793 (2017).
[6] A.A. Povzner, A.G. Volkov, T.A. Nogovitsyna. Physica B: Condens. Matter **536**, 408 (2018). https://doi.org/10.1016/j.physb.2017.10.112
[7] A.A. Povzner, A.G. Volkov, I.A. Yasyulevich. FTT **58**, 1283 (2016). (in Russian).
[8] M. Brando, D. Belitz, F.M. Grosche, T.R. Kirkpatrick. Rev. Mod. Phys. **88**, 25006 (2016). https://doi.org/10.1103/RevModPhys.88.025006
[9] A. Neubauer, C. Pfleiderer, B. Binz, A. Rosch, R. Ritz, P.G. Niklowitz, P. Böni. Phys. Rev. Lett. **102**, 186602 (2009).

[10] M.A. Wilde, M. Dodenhöft, A. Niedermayr, A. Bauer, M.M. Hirschmann, K. Alpin, A.P. Schnyder, C. Pfleiderer. Nature **594**, 374 (2021).
[11] C. Pappas, E. Leliévre-Berna, P. Falus, P.M. Bentley, E. Moskvin, S. Grigoriev, P. Fouquet, B. Farago. Phys. Rev. Lett. **102**, 197202 (2009).
[12] T. Moria. Spivoviye fluktuatsii v magnetikakh s kollektivizirovannymi elektronami. Mir, M. (1988), 288 s. (in Russian).
[13] A.A. Abrikosov, L.P. Gorkov, I.E. Dzyaloshinskiy. Metody kvantovoy teorii polya v statisticheskoy fizike. Fizmatgiz, M. (1962), 444 s. (in Russian).
[14] M.G. Vergniory, L. Elcoro, C. Felser, N. Regnault, B.A. Bernevig, Z. Wang. Nature **566**, 480 (2019). https://doi.org/10.1038/s41586-019-0954-4
[15] Y. Luo, S. Lin, D.M. Fobes, Z. Liu, E.D. Bauer, J.B. Betts, A. Migliori, J.D. Yhompson, M. Janoshek, B. Maiorov. Phys. Rev. B **97**, 104423 (2018).
[16] A.A. Povzner, A.G. Volkov, T.M. Nuretdinov. J. Magn. Magn. Mater. **507**, 166826 (2020).
[17] A.A. Povzner, A.G. Volkov, M.A. Chernikova, T.A. Nogovitsyna. Solid State. Commun. **371**, 115279 (2023).

Translated by I.Mazurov